

The upper critical field and its anisotropy in LiFeAs

J. L. Zhang,¹ L. Jiao,¹ F. F. Balakirev,² X. C. Wang,³ C. Q. Jin,³ and H. Q. Yuan^{1,*}

¹*Department of Physics, Zhejiang University, Hangzhou, Zhejiang 310027, China*

²*NHMFL, Los Alamos National Laboratory, MS E536, Los Alamos, NM 87545, USA*

³*Beijing National Laboratory for Condensed Matter Physics,*

Institute of Physics, Chinese Academy of Science, Beijing, 100080, China

(Dated: April 20, 2022)

The upper critical field $\mu_0 H_{c2}(T_c)$ of LiFeAs single crystals has been determined by measuring the electrical resistivity using the facilities of pulsed magnetic field at Los Alamos. We found that $\mu_0 H_{c2}(T_c)$ of LiFeAs shows a moderate anisotropy among the layered iron-based superconductors; its anisotropic parameter γ monotonically decreases with decreasing temperature and approaches $\gamma \simeq 1.5$ as $T \rightarrow 0$. The upper critical field reaches 15T ($H \parallel c$) and 24.2T ($H \parallel ab$) at $T = 1.4$ K, which value is much smaller than other iron-based high T_c superconductors. The temperature dependence of $\mu_0 H_{c2}(T_c)$ can be described by the Werthamer-Helfand-Hohenberg (WHH) method, showing orbitally and (likely) spin-paramagnetically limited upper critical field for $H \parallel c$ and $H \parallel ab$, respectively.

PACS numbers: 74.25.Op; 71.35.Ji; 74.70.Xa

I. INTRODUCTION

The discovery of superconductivity in iron pnictides¹ has attracted world-wide interests in searching for new type of high T_c superconductors and unveiling their unconventional nature of superconductivity. Until now, several series of iron-based superconductors have been found^{2,3}, which possess a similar layered crystal structure to those of the high T_c cuprates. Resembling the cuprates and heavy fermions, superconductivity in most of the iron pnictides/chalcogenides seems to be closely tied up with magnetism^{2,3}; superconductivity appears while antiferromagnetism is suppressed by hole (or electron) doping or by application of external pressure. In particular, the layered crystal structure and the high superconducting transition temperatures of the iron pnictides/chalcogenides initially suggested a strong analogy with the cuprates, providing an alternative to study the puzzles of high T_c superconductivity. However, significant discrepancies have been observed between the iron-based superconductors and other layered superconductors. For example, d-wave superconductivity was realized in the high T_c cuprates, but an s_{\pm} -type order parameter has been proposed for the iron pnictides/chalcogenides superconductors⁴⁻⁶. Upper critical field is another important superconducting parameter. A large upper critical field has been identified in both iron pnictides/chalcogenides and the cuprates, but the former shows a rather weak effect of anisotropy⁷⁻⁹. In particular, nearly isotropic upper critical field $\mu_0 H_{c2}(T_c)$ has been observed in the 122- and 11-type iron pnictides/chalcogenides^{7,8}, remarkably different from any other layered superconductors. LiFeAs, a much cleaner compound with a large ratio of room temperature resistivity to residual resistivity ($RRR \sim 40$), seems to be very unique among the iron pnictide superconductors¹⁰⁻¹². Bearing a nearly identical structure of $(\text{Fe}_2\text{As}_2)^{2-}$ and also a similar electronic structure

to other iron pnictides¹³, LiFeAs, however, shows simple metallic behavior prior to entering the superconducting state, lacking evidence of structural/magnetic transitions. Moreover, the stoichiometric compound LiFeAs becomes superconducting at ambient pressure and without introducing additional charge carriers via doping. Nevertheless, LiFeAs still demonstrates a relatively high T_c ($T_c \simeq 18$ K), being comparable with those iron pnictides/chalcogenides which parent compounds undergo a magnetic/structural transition. Unfortunately, LiFeAs is extremely air sensitive and many of its superconducting properties remain mysterious because of the restrictions of accessible experimental methods. In LiFeAs the extrapolation of $\mu_0 H_{c2}$ near T_c to zero temperature gives a rather large value of $\mu_0 H_{c2}(0) (\sim 80 \text{ T})$ ¹². In order to fully track the field dependence of superconductivity, a strong magnetic field is desired. Here we report the first resistivity measurement of LiFeAs in a pulsed magnetic field down to 1.4K, from which the temperature-magnetic field phase diagram is well established. The upper critical field $\mu_0 H_{c2}$ is determined to be 15 T and 24.2 T at $T = 1.4$ K for $H \parallel c$ and $H \parallel ab$, respectively. In comparison with other series of iron pnictide superconductors, the upper critical field shows a moderate anisotropic effect and its value of $\mu_0 H_{c2}(0)$ is largely reduced.

II. EXPERIMENTAL METHODS

High-quality single crystals of LiFeAs have been grown by a self-flux technique¹⁰. The precursor of Li_3As was synthesized from Li piece and As chips that were sealed in a Nb tube under Ar atmosphere and then treated at 650°C for 15 hours in a sealed quartz tube. The Li_3As , Fe and As powders were mixed in the ratio of Li:Fe:As=1:0.8:1. The powder mixture was then pressed into a pallet in an alumina oxide tube. To prevent the vaporized Li from attacking the quartz tube at high tem-

perature, the sample pallet was subsequently sealed in a Nb tube and a quartz tube under vacuum. The sealed quartz tube was heated at 800°C for 10h before heating up to 1100 °C at which it was held for another 10h. Finally, it was cooled down to 800°C with a rate of 5°C per hour. Crystals with a size up to 4mm×3mm×0.5mm were obtained. The whole preparation work were carried out in a glove box protected with high purity Ar gas. The obtained single crystals were first characterized by x-ray diffraction with a Mac Science diffractometer and ac susceptibility measurements using the Oxford cryogenic system (Maglab-Exa-12) prior to the transport measurements in a pulsed magnetic field at Los Alamos.

Electrical resistivity was measured using a typical four-contact method in pulsed fields of up to 40T and at temperatures down to 1.4K in a Helium-4 cryostat. Note that the applied electrical current was always along the ab-plane. In order to minimize the inductive self-heating caused by the fast change of magnetic field, small crystals with typical sizes 2mm ×0.5mm×0.1mm were cleaved off along the c-direction from the as-grown samples. In order to avoid oxidizing the samples, special cares were paid to protect the samples from exposing to air while preparing for the electrical contacts. Data were recorded using a 10 MHz digitizer and 100 kHz alternating current, and analyzed using a custom low-noise digital lock-in technique. Temperature dependence of the electrical resistivity at zero field was measured with a Lakeshore resistance bridge.

III. EXPERIMENTAL RESULTS AND DISCUSSION

Fig. 1 presents the temperature dependence of the electrical resistivity $\rho(T)$ at zero magnetic field for LiFeAs. Obviously, LiFeAs shows simple metallic behavior upon cooling down from room temperature, followed

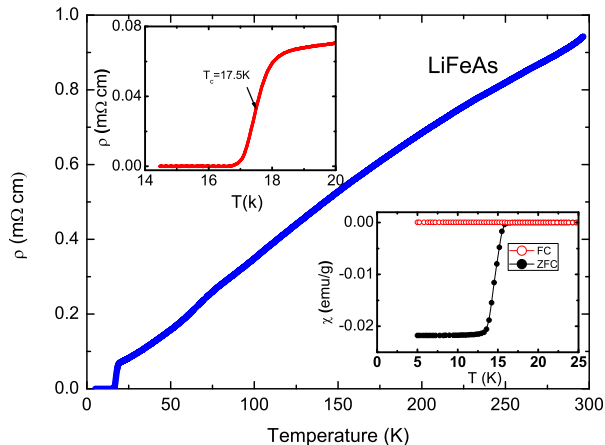


FIG. 1: Temperature dependence of the electrical resistivity $\rho(T)$ for LiFeAs at zero field. The lower inset shows the magnetic susceptibility $\chi(T)$.

by a sharp superconducting transition at $T_c \simeq 17.5$ K, which is in consistence with the reports in literature^{10–12}. Note that the weak kink in the resistivity $\rho(T)$ around 75K is attributed to the change of cooling rate. No evidence of structural/magnetic transition has been observed in LiFeAs. In order to demonstrate the superconducting transition in detail, we plot the low temperature electrical resistivity and magnetic susceptibility in the inset of Fig.1, which were measured with samples cut from the same batch. As frequently observed in superconductors, the bulk T_c determined from the magnetic susceptibility is slightly lower. The observations of a large RRR ($\simeq 15$) and a narrow superconducting transition indicate high quality of the samples investigated here. Since LiFeAs is a good metal with low resistivity, measurements of its electrical resistivity in a pulsed magnetic field is rather challenging. Nevertheless, we have succeeded in obtaining a good set of resistivity data up to a magnetic field of 40T after many failures. Fig. 2 shows the field dependence of the electrical resistivity $\rho(\mu_0 H)$ of LiFeAs at variant temperatures, in which the magnetic field is applied along (a) the c-axis and (b) the ab-plane, respectively. One can see that a relatively sharp superconducting transition survives down to very low temperatures, even though the signals become more noisy upon cooling down, in particular for the case of $H \parallel ab$. Obviously, the superconducting transition is eventually suppressed upon applying a magnetic field, but the critical field required to suppress superconductivity is much larger for

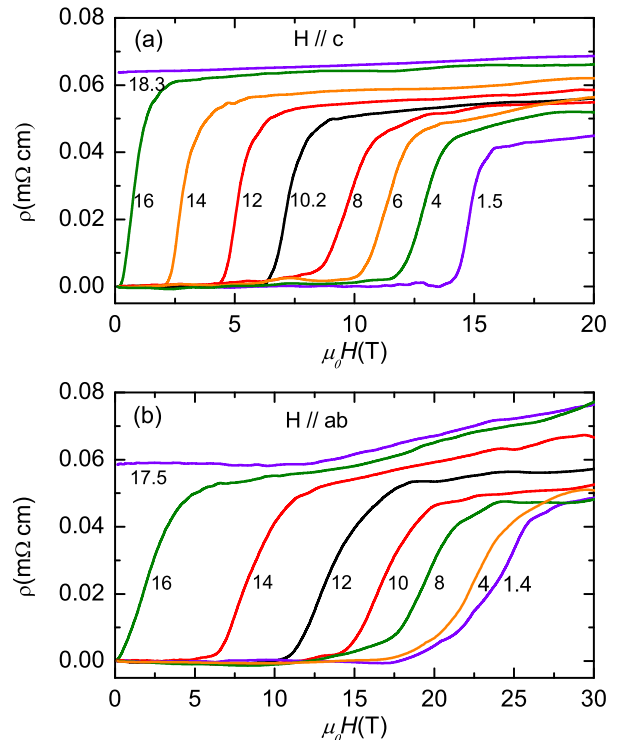


FIG. 2: Magnetic field dependence of the electrical resistivity at variant temperatures for LiFeAs: (a) $H \parallel c$; (b) $H \parallel ab$.

$H \parallel ab$. Furthermore, the normal state of LiFeAs remains metallic upon suppressing superconductivity in a sufficiently high magnetic field, being different from those of the 122- and 11-type compounds^{7,8}.

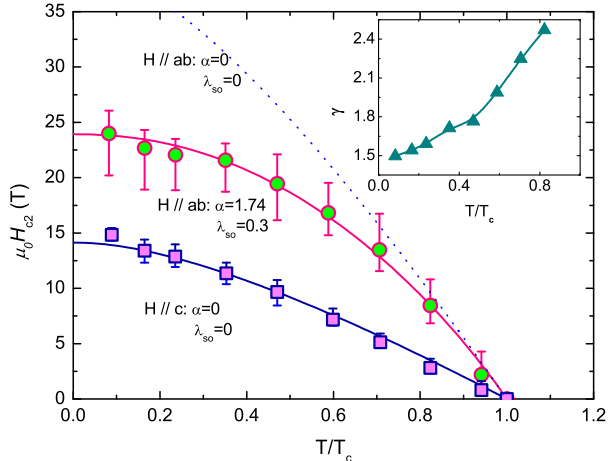


FIG. 3: The upper critical field $\mu_0 H_{c2}(T_c)$ and the corresponding WHH fits for LiFeAs. The solid lines are the best fits to the experimental data and the dotted line is the WHH fit without considering the spin paramagnetic effect. The inset shows the temperature dependence of the anisotropic parameter γ .

The upper critical field $\mu_0 H_{c2}(T_c)$ of LiFeAs, determined from the mid-point of the superconducting transition, is plotted in Fig. 3. The error bars were derived from the 20% and 80% drop of the normal state resistivity at T_c . In comparison with other families of the iron-based high temperature superconductors⁷⁻⁹, LiFeAs shows a relatively small upper critical field, reaching $\mu_0 H_{c2}=15\text{T}$ and 24.2T at $T = 1.4\text{K}$ for $H \parallel c$ and $H \parallel ab$, respectively. Temperature dependence of the anisotropic parameter, defined as $\gamma = H_{c2}^{H \parallel ab} / H_{c2}^{H \parallel c}$, is plotted in the inset of Fig.3. Resembling those of the previously investigated iron-based superconductors⁷⁻⁹, the anisotropic parameter γ decreases with decreasing temperature, reaching $\gamma = 1.5$ at zero temperature. Such a value of γ is slightly higher than that of the 122- and 11-type compound^{7,8}, which shows nearly isotropic behavior at low temperatures, but significantly smaller compared to that of the high T_c cuprates and organic superconductors^{14,15}. According to the Werthamer-Helfand-Hohenberg method¹⁶, the upper critical field limited by the orbital mechanisms in the dirty limit is given by:

$$\mu_0 H_{c2}^{orb}(0)[\text{T}] = -0.69 T_c (dH_{c2}/dT)|_{T=T_c} [\text{K}]. \quad (1)$$

On the other hand, superconductivity is suppressed while the magnetic energy associated with the Pauli spin susceptibility in the normal state exceeds the condensation energy in the superconducting state as a result of Zeeman effect. In this case, the Pauli-limited upper

critical field for weakly coupled superconductors can be written as^{17,18}:

$$\mu_0 H_{c2}^P(0)[\text{T}] = 1.86 T_c [\text{K}]. \quad (2)$$

For conventional superconductors, $\mu_0 H_{c2}^P(0)$ is usually much larger than $\mu_0 H_{c2}^{orb}(0)$ and, therefore, their upper critical field is mainly restricted by the orbital pair-breaking mechanism. In our case, the initial slope of $\mu_0 H_{c2}$ at T_c , i.e., $-d\mu_0 H_{c2}/dT|_{T=T_c}$, is determined as 3.3 T/K and 1.2 T/K for $H \parallel ab$ and $H \parallel c$, respectively. Thus the values of $\mu_0 H_{c2}^P(0)$ are accordingly derived as 39.8T for $H \parallel ab$ and 14.5T for $H \parallel c$; the latter is close to the experimental value of $\mu_0 H_{c2} \simeq 15\text{T}$ at $T = 1.4\text{K}$, indicating an orbitally limited critical field for $H \parallel c$. On the other hand, Eq. 2 yields $\mu_0 H_{c2}^P(0) = 32.6\text{T}$. The experimentally derived value of $\mu_0 H_{c2}(0) \sim 25\text{T}$ for $H \parallel ab$ is, therefore, well below the corresponding values of $\mu_0 H_{c2}^{orb}(0)$ and $\mu_0 H_{c2}^P(0)$. The solid lines in Fig. 3 present the WHH fits to the experimental data of $\mu_0 H_{c2}(T_c)$, in which both the spin-paramagnetic and orbital pair-breaking effects were considered¹⁶. The parameter λ_{so} describes the strength of the spin-orbit scattering. The fits give the Maki parameter $\alpha = 0$ and 1.74 for field along the c-axis and the ab-plane, respectively. The former further confirms the orbitally limited critical field for $H \parallel c$. However, the resulted fitting parameters ($\alpha = 1.74$, $\lambda_{so} = 0.3$) indicate that the upper critical field is likely spin-paramagnetically limited for $H \parallel ab$ even though we still could not exclude the possibility of the orbital effect due to its multi-band effect. As shown in Fig. 3 (see the dotted line and the solid line for $H \parallel ab$), the spin-paramagnetic effect might lower the upper critical field, and therefore, reduce the anisotropy of $\mu_0 H_{c2}$ at low temperatures. For comparison, Fig. 4 plots the

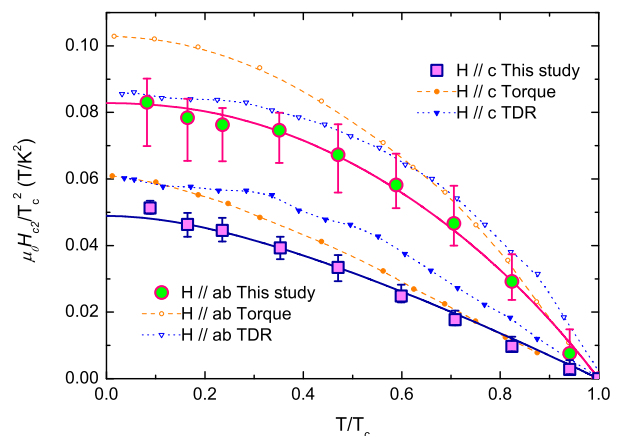


FIG. 4: The scaled upper critical field $\mu_0 H_{c2}(T_c)/T_c^2$ versus the normalized temperature T/T_c for LiFeAs. Symbols of the square (\square), circle (\circ) and triangle (∇) represent the data obtained from measurements of the electrical resistivity (this study), the magnetic torque¹⁹ and the resonant frequencies based on the tunnel-diode oscillator (TDR)²⁰, respectively.

TABLE I: The derived superconducting parameters for LiFeAs

field	T_c (K)	$-\frac{d\mu_0 H_{c2}}{dT} _{T_c}$ (T/K)	$\mu_0 H_{c2}(1.4K)$ (T)	$\mu_0 H_{c2}^{orb}$ (T)	$\mu_0 H_{c2}^P$ (T)	α	λ_{so}	ξ (nm)
$H \parallel c$	17.5	1.2	15	14.5	32.6	0	0	1.7
$H \parallel ab$	17.5	3.3	24.2	39.8	32.6	1.74	0.3	4.8

available upper critical fields for LiFeAs, independently determined from measurements of the electrical resistivity (this work), the magnetic torque¹⁹ and the resonant frequencies based on a tunnel-diode oscillator²⁰. One can see that the experimental results obtained from the above three methods are similar in general; the visible discrepancy might result from the exact determination of T_c . Nevertheless, the electrical resistivity studied here provides the most direct approach for determining the upper critical field.

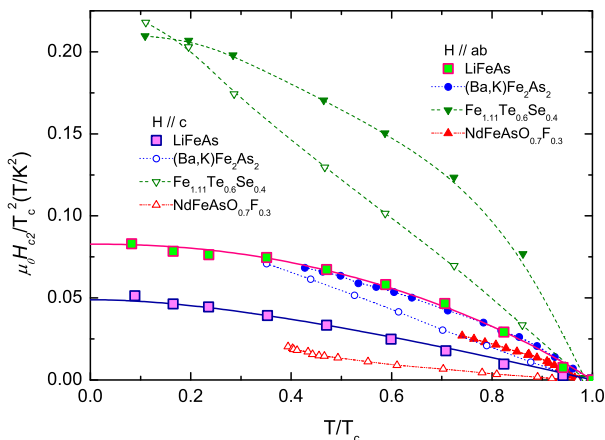


FIG. 5: The upper critical field $\mu_0 H_{c2}/T_c^2$ versus the normalized temperature T/T_c for single crystals of LiFeAs (this study), $(\text{Ba,K})\text{Fe}_2\text{As}_2$ ⁷ and $\text{Fe}_{1.11}\text{Te}_{0.6}\text{Se}_{0.4}$ ⁸, $\text{NdFeAsO}_{0.7}\text{F}_{0.3}$ ⁹, which $T_c=17.5\text{K}$, 55K , 28K and 14K , respectively. Note that variant symbols represent variant compounds as marked in the figure.

In Fig. 5, we compare the upper critical field and its anisotropy in several typical iron-based superconductors, i.e., LiFeAs (this work), $(\text{Ba,K})\text{Fe}_2\text{As}_2$ ⁷ and $\text{Fe}_{1.11}\text{Te}_{0.6}\text{Se}_{0.4}$ ⁸, $\text{NdFeAsO}_{0.7}\text{F}_{0.3}$ ⁹. In general, the upper critical fields of all these compounds show a rather weak anisotropy at low temperatures in comparison with other layered superconductors, e.g., the high T_c cuprates and the organic superconductors^{14,15}. This indicates that the inter-layer coupling might become significantly important in the iron-based superconductors, which was ignored while modeling the high T_c cuprates. Among the iron-based superconductors, LiFeAs shows a relatively

small upper critical field. For example, $\text{Fe}_{1.11}\text{Te}_{0.6}\text{Se}_{0.4}$ undergoes a superconducting transition at $T_c \simeq 14\text{K}$, but it shows a much larger upper critical field ($\mu_0 H_{c2}(0) \simeq 45\text{T}$), which is likely attributed to its higher disorder. In $(\text{Ba,K})\text{Fe}_2\text{As}_2$ and $\text{Fe}_{1.11}\text{Te}_{0.6}\text{Se}_{0.4}$ systems^{7,8}, we observed a nearly isotropic upper critical field at low temperature, which unique feature was attributed to the three-dimensional-like Fermi surface as experimentally confirmed later²¹. The moderate anisotropy of $\mu_0 H_{c2}$ in LiFeAs and the 1111-series is actually consistent with the band structure calculations which indicate an enhanced anisotropy in these systems¹³.

IV. CONCLUSION

In summary, we have determined the complete temperature-magnetic field phase diagram for the superconductor LiFeAs by means of measuring the electrical resistivity in a field up to 40T. The upper critical field of LiFeAs is derived as $\mu_0 H_{c2}(1.4\text{K})=15\text{T}$ and 24.2T for field applied along the c -axis and the ab -plane, respectively. The anisotropic parameter γ decreases with decreasing temperature and shows a weak anisotropic effect at low temperatures. These findings indicate that weak anisotropy of $\mu_0 H_{c2}$ seems to be a common feature of the iron-based superconductors, in spite of the layered nature of their crystal structure.

V. ACKNOWLEDGEMENTS

This work was supported by the National Science Foundation of China (No.10874146 and No. 10934005), the National Basic Research Program of China (973 program) under grant No. 2011CBA00103 and 2009CB929104, the PCSIRT of the Ministry of Education of China, Zhejiang Provincial Natural Science Foundation of China and the Fundamental Research Funds for the Central Universities. Work at NHMFL-LANL is performed under the auspices of the National Science Foundation, Department of Energy and State of Florida.

* Electronic address: hqyuan@zju.edu.cn

¹ Y. Kamihara, T. Watanabe, M. Hirano, and H. Hosono, J. Am. Chem. Soc. **130**, 3296 (2008).

² Z. A. Ren, and Z. X. Zhao, Adv. Mat. **21**, 4584 (2009).

³ M. D. Lumsden, and A. D. Christianson, J. Phys.: Condens. Matter **22**, 203203 (2010).

- ⁴ K. Seo, B. A. Bernevig, and J. P. Hu Phys. Rev. Lett. **101**, 506404 (2008).
- ⁵ I. I. Mazin, D. J. Singh, M. D. Johannes, and M. H. Du, Phys. Rev. Lett. **101**, 057003 (2008).
- ⁶ T. Hanaguri, S. Niitaka, K. Kuroki, and H. Takagi, Science **328**, 474 (2010).
- ⁷ H. Q. Yuan, J. Singleton, F. F. Balakirev, S. A. Baily, G. F. Chen, J. L. Luo and N. L. Wang, Nature(London) **457**, 565 (2009).
- ⁸ M. H. Fang, J. H. Yang, F. F. Balakirev, Y. Kohama, J. Singleton, B. Qian, Z. Q. Mao, H. D. Wang and H. Q. Yuan, Phys. Rev. B **81**, 20509 (2010).
- ⁹ J. Jaroszynski, F. Hunte, L. Balicas, Y. Jo, I. Raicevic, A. Gurevich, D. C. Larbalestier, F. F. Balakirev, L. Fang, P. Cheng, Y. Jia, and H. H. Wen, Phys. Rev. B **78**, 174523 (2008).
- ¹⁰ X. C. Wang, Q. Q. Liu, Y. X. Lv, W. B. Gao, L. X. Yang, R. C. Yu, F. Y. Li, and C. Q. Jin, Solid State Commun. **148**, 538 (2008).
- ¹¹ J. H. Tapp, Z. Tang, B. Lv, K. Sasmal, B. Lorenz, P. C. W. Chu, and A. M. Guloy, Phys. Rev. B **97**, 060505 (2008).
- ¹² Y. J. Song, J. S. Ghim, B. H. Min, Y. S. Kwon, H. M. Jung, and J-S. Rhyee, Appl. Phys. Lett. **96**, 212508 (2010).
- ¹³ I. A. Nekrasov, Z. V. Pchelkina, and M. V. Sadovskii, J. Exp. Theor. Phys. Letters. **88**, 543 (2008).
- ¹⁴ J. R. Shrieffer, and J. S. Brooks, Handbook of High-Temperature Superconductivity (Springer, 2006).
- ¹⁵ J. Singleton and C. Mielke, Contemp. Phys. **43**, 63 (2002).
- ¹⁶ N. R. Werthamer, E. Helfand, and P. C. Hohenberg, Phys. Rev. **147**, 295 (1966).
- ¹⁷ A. M. Clogston, Phys. Rev. Lett. **9**, 266 (1962).
- ¹⁸ B. S. Chandrasekhar, J. Appl. Phys. Lett. **1**, 7 (1962).
- ¹⁹ N. Kurita, K. Kitagama, K. Matsubayashi, A. Kismarhardja, E-S. Choi, J. S. Brooks, Y. Uwatoko, S. Uji, and T. Terashima, J. Phys. Soc. Jpn. **80**, 013706 (2011).
- ²⁰ K. Cho, H. Kim, M. A. Tanatar, Y. J. Song, Y. S. Kwon, W. A. Coniglio, C. C. Agosta, A. Gurevich, and R. Prozorov, arXiv: cond-mat/1011.5126v2 (2010).
- ²¹ P. Vilmercati, A. Fedorov, I. Vobornik, U. Manju, G. Panaccione, A. S. Goldoni, A. S. Sefat, M. A. McGuire, B. C. Sales, R. Jin, D. Mandrus, D. Singh, and N. Manella, Phys. Rev. B **79**, 220503 (2009).